0026-895X/99/060982-11$3.00/0

MOLECULAR PHARMACOLOGY, **55:**982–992 (1999).

Effect of Mutations within the Peripheral Anionic Site on the Stability of Acetylcholinesterase

NATHALIE MOREL, SUZANNE BON, HARRY M. GREENBLATT, DANIEL VAN BELLE, SHOSHANA J. WODAK, JOEL L. SUSSMAN, JEAN MASSOULIÉ, AND ISRAEL SILMAN

Laboratoire de Neurobiologie Cellulaire et Moléculaire, Centre National de la Recherche Scientifique, Unité de Recherche Mixte 8544, Ecole Normale Supérieure, Paris, France (N.M, S.B., J.M., I.S.); Departments of Structural Biology (H.M.G., J.L.S.) and Neurobiology (I.S.), Weizmann Institute of Science, Rehovoth, Israel; and Unité de Conformation de Macromolécules Biologiques, Université Libre de Bruxelles, Bruxelles, Belgium (D.V.B., S.J.W.)

Received October 1, 1998; accepted February 12, 1999

This paper is available online at http://www.molpharm.org

ABSTRACT

Torpedo acetylcholinesterase is irreversibly inactivated by modifying a buried free cysteine, Cys231, with sulfhydryl reagents. The stability of the enzyme, as monitored by measuring the rate of inactivation, was reduced by mutating a leucine, Leu282, to a smaller amino acid residue. Leu282 is located within the "peripheral" anionic site, at the entrance to the active-site gorge. Thus, loss of activity was due to the increased reactivity of Cys231. This was paralleled by an increased susceptibility to thermal denaturation, which was shown to be due to a large decrease in the activation enthalpy. Similar results were obtained when either of two other residues in contact with Leu282 in *Torpedo* acetylcholinesterase, Trp279 and Ser291, was replaced by an amino acid with a smaller side chain. We studied the effects of various ligands specific for either the active or peripheral sites on both thermal inactivation and on inactivation by 4,4′-dithiodipyridine. The wild-type and mutated enzymes could be either protected or sensitized. In some cases, opposite effects of the same ligand were observed for chemical modification and thermal denaturation. The mutated residues are within a conserved loop, W279-S291, at the top of the active-site gorge, that contributes to the peripheral anionic site. Theoretical analysis showed that *Torpedo* acetylcholinesterase consists of two structural domains, each comprising one contiguous polypeptide segment. The W279-S291 loop, located in the first domain, makes multiple contacts with the second domain across the active-site gorge. We postulate that the mutations to residues with smaller side chains destabilize the conserved loop, thus disrupting cross-gorge interactions and, ultimately, the entire structure.

Torpedo acetylcholinesterase (AChE) contains a nonconserved cysteine residue, Cys231, buried within the protein, ca. 8 Å from the active-site serine, Ser200 (Sussman et al., 1991). Chemical modification of the free thiol group of this amino acid residue by a repertoire of sulfhydryl reagents causes irreversible inactivation of the enzyme, even when modification is reversible (Kreimer et al., 1994). Inactivation is due to an irreversible conformational transition of the native enzyme to a molten globule (MG) species (Kreimer et al., 1994). Modification, as well as concomitant inactivation, obeys pseudofirst order kinetics (Steinberg et al., 1990; Kreimer et al., 1994). The rate of modification by a given thiol reagent is much slower than for a reaction with a low-molecular-weight thiol, as reflected by the high activation energy of the reaction (Kreimer et al., 1994).

The Ellman reaction for assay of AChE (Ellman et al., 1961) involves the use of a thiol reagent, namely 5,5′-dithiobis(2-nitrobenzoic acid) (DTNB), also known as Ellman's reagent, which is reduced by the thiocholine generated by enzymic hydrolysis of acetylthiocholine (ATCh) to yield the chromophore 2-nitro-5-thiobenzoic acid. Nevertheless, *Torpedo* AChE can routinely be assayed by the Ellman method because the $T_{1/2}$ for its inactivation by DTNB at neutral pH and room temperature is approximately 9 h (Steinberg et al., 1990). Therefore, it was not anticipated that a mutant *Torpedo* AChE, L282S, generated by mutating Leu282, a leucine residue located close to the surface of the enzyme and near the mouth of the active-site gorge (Fig. 1; Sussman et al., 1991; Harel et al., 1995), to either serine or alanine, would be unstable under the conditions of the Ellman assay. This mutant had been generated to promote glycosylation of the adjacent residue, Asn280, by creating the glycosylation signal AsnXSer. However, instability was not due to glycosylation because the analogous mutant, L282A, displayed similar instability. With the following results, we demonstrate that

[1] For rat mutants, the residue number for the equivalent amino acid in *Torpedo* AChE is given in brackets, according to the accepted nomenclature (Massoulié et al., 1992).

ABBREVIATIONS: AChE, acetylcholinesterase; ATCh, acetylthiocholine; *Tc*AChE, *Torpedo californica* acetylcholinesterase; *Tm*AChE, *Torpedo marmorata* acetylcholinesterase; DTNB, 5,5′-dithiobis(2-nitrobenzoic acid); DTP, 4,4′-dithiodipyridine; MG, molten globule; WT, wild type.

such mutants, generated by replacement of Leu282 with a smaller residue, are, indeed, destabilized, and we present evidence that the instability observed under assay conditions derives from enhanced reactivity of Cys231 relative to its reactivity in the wild-type (WT) enzyme. This, in turn, is related to a decrease in the overall thermal stability of the mutant enzyme. Both the enhanced susceptibility to chemical modification and the decreased thermal stability can be modulated by reversible inhibitors specific for either the active site or the "peripheral" anionic site. Leu282 is within a loop stretching from Trp279 to Ser291. This loop is an important constituent of the peripheral anionic site (Harel et al., 1993, 1995; Bourne et al., 1995). It also contributes the principal hydrophobic stretch to a 5-kDa polypeptide, Gly268-Lys315, which serves to anchor a MG species of *Torpedo californica* AChE (*Tc*AChE) to liposomes (Shin et al., 1996). The peripheral anionic site of AChE has been shown to enhance the rate of amyloid fibril assembly from Aβ peptide (Inestrosa et al., 1996), and, more recently, the isolated polypeptide sequence has been shown to be endowed with this capacity (De Ferrari and Inestrosa, 1998). Thus, elucidation of the physicochemical forces governing the stability of the Trp279-Ser291 loop warrants further investigation.

Experimental Procedures

Materials. ATCh, DTNB, propidium iodide, gallamine triethiodide, *d*-tubocurarine, decamethonium bromide, 4,4′-dithiodipyridine (DTP), and BSA were all purchased from Sigma Chemical Co. (St. Louis, MO). Edrophonium chloride was obtained from Hoffman-La Roche (Basel, Switzerland). All salts and buffers were of analytical grade.

Site-Directed Mutagenesis and Transfection. The coding sequences of the H catalytic subunits of *Torpedo marmorata* AChE (*Tm*AChE; Duval et al., 1992) and of rat AChE (Legay et al., 1993) were inserted into the pEF-BOS vector and were mutagenized with oligonucleotide primers, as described previously (Duval et al., 1992). COS-7 cells were transfected as described previously (Duval et al., 1992). After transfection, the COS cells were incubated for 2 days at 37°C and then for 4 days at 27°C in the case of the *Torpedo* enzyme, and incubated for 4 days at 37°C in the case of rat AChE.

AChE Activity Assays. AChE activity was determined by the colorimetric method of Ellman et al. (1961) at room temperature, with 0.75 mM ATCh as the substrate, in 50 mM sodium phosphate (pH 7.4) containing 0.5 mM DTNB and 0.1 mg/ml BSA. Assays were performed in microplates with a Labsystems (Helsinki, Finland) Multiskan RC automatic plate reader and recording at 414 nm every 20 s. K_m values were determined under the same experimental conditions in a concentration range of 0.02 to 10 mM ATCh, and IC_{50} values were determined with 0.5 mM ATCh. AChE samples were preincubated with the inhibitors in the reaction mixture for 20 min before the initiation of the enzymic reaction by addition of the substrate.

Inactivation by DTP. Chemical inactivation was performed in buffer 1 (0.01% BSA/40 mM NaCl/10 mM Tris hydrochloride; pH 7.4) containing 1 mM DTP in the case of *Tm*AChE and 0.05 mM DTP for the rat enzyme. Ten-microliter aliquots of the appropriate AChE sample were added to 100 μl of the DTP-containing buffer, which was then incubated at 26.5°C. At appropriate time intervals, 10-μl aliquots were withdrawn and stored on ice for up to 1 h before assay of residual activity.

Thermal Inactivation. Thermal inactivation experiments were performed by the addition of 10-μl aliquots of the appropriate AChE sample to 100 μl of buffer 1, which was then brought to the appropriate temperature. Arrhenius plots were determined from the initial rates of loss of enzymic activity at four appropriate temperatures for each AChE sample, assuming that thermal denaturation obeys first order kinetics, yielding values of $\Delta H^{\ddagger}$.

Software. Domain limits were computed from the atomic coordinates of the free *Tc*AChE molecule (Protein Data Bank entry 2ace) by a recently developed procedure (Wernisch et al., 1999) that uses a graph heuristic to partition the protein into sets of residues that

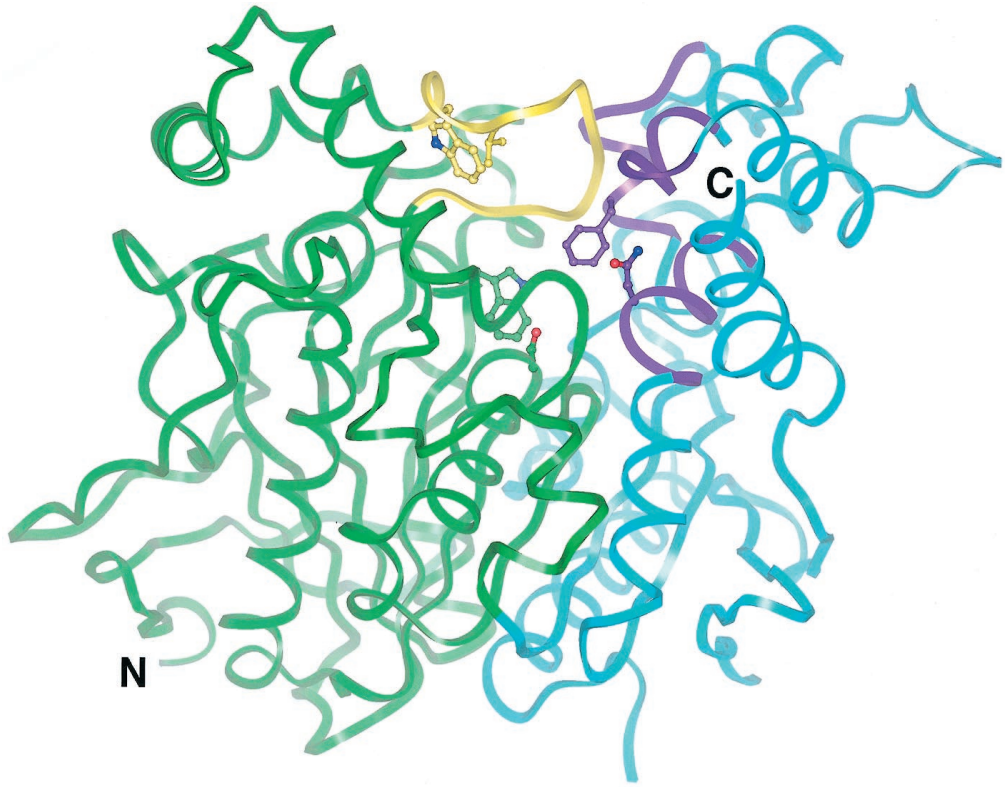

Fig. 1. Ribbon diagram of *Tc*AChE. Residues 4 to 305 are colored green, and residues 306 to 535 are colored cyan, highlighting the division of the molecule into two putative domains. The loop containing Leu282, viz. Trp279-Ser291, is colored yellow, with the side chains of Trp279 and Leu282 represented in stick form. The three regions of the second domain of the molecule that interact with this loop are colored purple, and two side chains, Phe 331 and Asn399, are shown in stick form. The active-site residues, Trp84 and Ser200, at the bottom of the active-site gorge, are also shown in stick form to provide orientation (picture was made in Insight II).

display minimum interactions between them. The interactions are evaluated from the contact areas between atoms, which are computed from the weighted Voronoi diagram (Richards, 1974). The accessible surface areas of residues in the protein and the area buried in the interface between the two domains were evaluated with the program SurVol (Alard, 1992). All of the procedures use a probe size of 1.4 Å for the water molecule and the set of radii implemented in the BRUGEL package (Delhaise et al., 1984).

The programs Insight II (MSI Corp. San Diego, CA) and XtalView (McRee, 1992) were used for display and analysis, and Raster3D (Merritt and Bacon, 1997) was used to render some of the images used in this study. The Collaborative Computational Project, Number 4 program (1994), CONTACT, was used to assess interdomain contacts.

Results

Figure 2 displays the enzymic activity of aliquots of WT *Tm*AChE and of the corresponding L282S mutant as a function of time, at 30°C, under standard Ellman assay conditions (see *Experimental Procedures*). Whereas the activity of the WT enzyme, as expected, decreases only slightly over 15 min, that of the L282S mutant decays significantly. In addition, the effects of the two peripheral site ligands, *d*-tubocurarine and gallamine (Changeux, 1966), should be noted. Whereas the addition of 0.4 mM gallamine stabilizes L282S over the period monitored, *d*-tubocurarine (50 μM) substantially enhances the rate at which its enzymic activity decays. Propidium, like gallamine, stabilizes the L282S mutant (not shown). Neither *d*-tubocurarine nor gallamine had a significant effect on the slow loss of activity of WT *Tm*AChE.

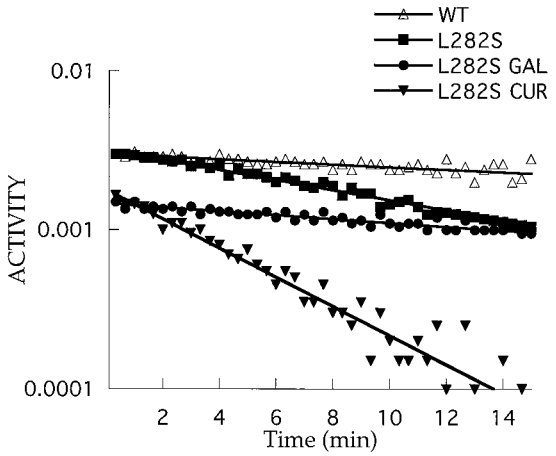

Fig. 2. Catalytic activity of WT and of L282S *Tm*AChE as a function of time under standard assay conditions. Catalytic activity was measured under standard assay conditions (see *Experimental Procedures*). The activity at a given time was calculated from the change in optical density of the reaction mixture over a time interval of 20 s. The change with time in the catalytic activity of the L282 mutant was also monitored in the presence of *d*-tubocurarine (50 μM) and of gallamine (0.4 mM).

Our earlier studies of chemical modification and concomitant deactivation of *Tc*AChE by thiol reagents (Steinberg et al., 1990; Kreimer et al., 1994) suggested that the instability of L282S under the conditions of the Ellman assay might have its origin in the enhanced reactivity of Cys231 in the mutant enzyme relative to the WT enzyme. Therefore, this possibility was examined directly. Figure 3 shows the results of experiments in which samples of WT *Tm*AChE and of various mutant enzymes were preincubated in the presence of the disulfide DTP (Kreimer et al., 1994) before assay by the Ellman procedure. Both L282S (not shown) and the analogous mutant, L282A, are stable in the absence of DTP at

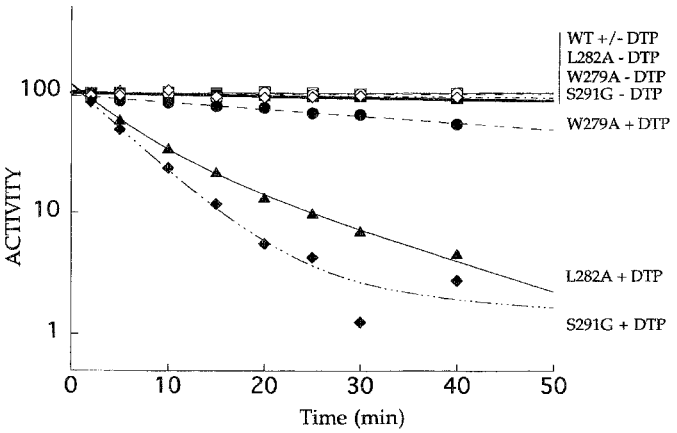

Fig. 3. Kinetics of inactivation of WT and of mutant *Tm*AChE by DTP. Inactivation was performed at 26.5°C. Ten-microliter aliquots of the *Tm*AChE sample were added to 100 μl of 1 mM DTP in buffer 1. At appropriate time intervals, 10-μl aliquots were withdrawn and stored on ice for up to 1 h before assay of residual enzymic activity.

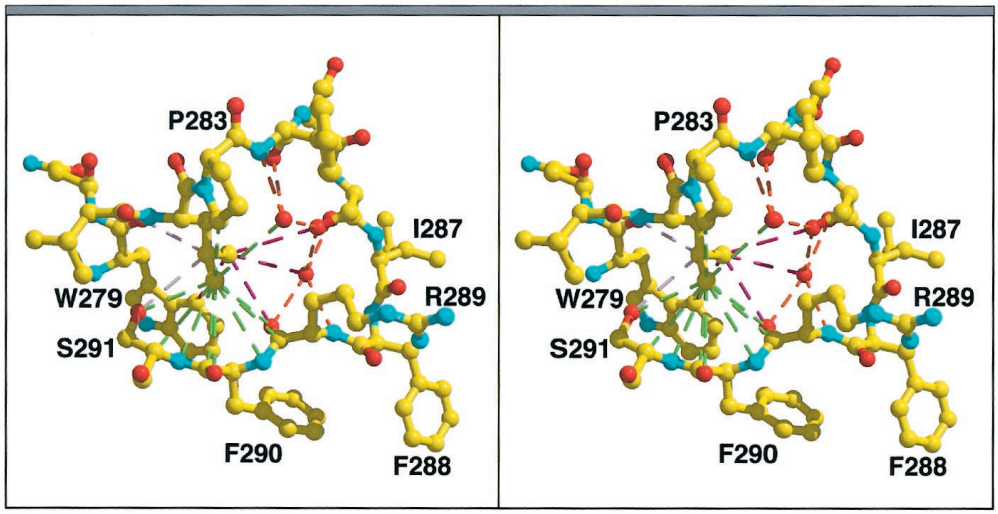

Fig. 4. Stereo view of the Trp279-Ser291 loop. Contacts made by the side chain atoms of Leu282 are shown by dashed lines: mauve for C^{γ}, green for $C^{\delta 1}$, and purple for $C^{\delta 2}$. Red dashed lines represent possible hydrogen bonds between the two water molecules shown (red spheres) and protein atoms. Wat580 is the uppermost of the two and Wat584 is below. The orientation in this figure is similar to that in Fig. 1 (picture was made in XtalView/Raster3D).

26.3°C, but unstable in its presence, with $T_{1/2}$ values of ca. 7 min under the experimental conditions used. WT *Tm*AChE is stable under the same conditions, as is the double-mutant C231S/L282A, which lacks the free thiol of Cys231 (not shown). The fact that the L282A mutant is destabilized to a similar extent as the L282S mutant shows that destabilization is not due to glycosylation. This was confirmed by the fact that the N280Q/L282S double mutant was also unstable in the presence of DTP (not shown).

Inspection of the three-dimensional structure of *Torpedo* AChE (see *Discussion*) revealed that the side chain of Leu282 makes contact principally with the side chains of two other residues, the indole ring of Trp279 and the hydroxyl group of Ser291 (Fig. 4). Thus, it was of interest to see whether substitution of either of these two residues by amino acids with smaller side chains would reduce the stability of *Tm*AChE in a similar manner. Accordingly, two appropriate mutants, W279A and S291G, were generated, and Fig. 3 shows that these mutations also increase susceptibility to DTP. The degree of susceptibility produced by the S291G mutation is similar to or greater than that produced by the L282S/A mutation, whereas that produced by the W279A mutation is much smaller.

The instability of all three mutants relative to WT *Tm*AChE, as monitored by susceptibility to chemical modification, was paralleled by reduced thermal stability. Thus, WT *Tm*AChE was fairly stable at 38°C and pH 7.75, losing ca. 10% of its activity in 3 h. Under the same conditions, the L282A, S291G, and W279A mutants displayed $T_{1/2}$ values of ca. 25 min, 6 min, and 256 min, respectively. Arrhenius plots showed that the decreased thermal stability was due to large decreases in the activation energy, from 170 kcal/mol for WT enzyme to 100 kcal/mol and 90 kcal/mol, respectively, for the L282A and S291G mutants (Fig. 5). A smaller decrease, to 135 kcal/mol, was observed for the W279A mutant, paralleling its more limited sensitivity to DTP. Figure 5 also shows

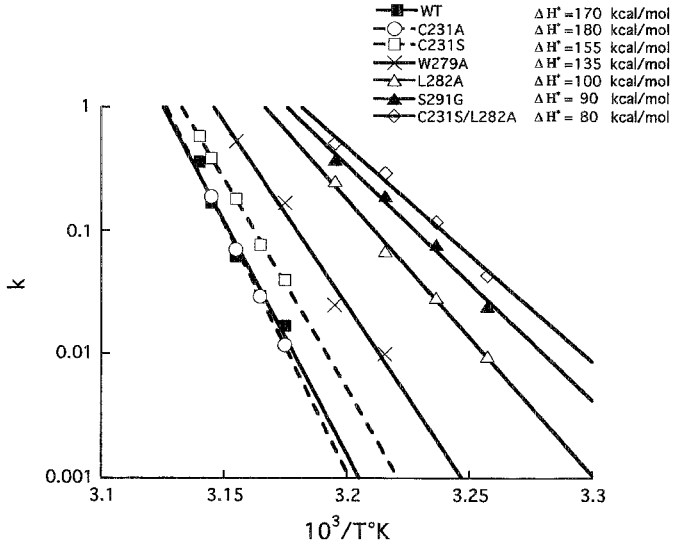

Fig. 5. Activation energies for thermal denaturation of WT and mutant *Tm*AChEs. Arrhenius plots were derived from the experimental data for the kinetics of thermal inactivation at four temperatures for each AChE sample. A 10-μl aliquot of the *Tm*AChE sample was added to 100 μl of buffer 1 before incubation at the desired temperature. At suitable time intervals, 10-μl aliquots were withdrawn and stored on ice for up to 1 h before assay of residual enzymic activity.

that the C231S mutant is slightly less stable than the WT and that the C231S/L282S double mutant is slightly less stable than L282S, which is in agreement with the observations of Wilson et al. (1996).

Vertebrate AChE displays a high degree of conservation, with *Torpedo* AChE possessing ca. 50% sequence identity and ca. 70% sequence similarity to various mammalian AChEs (Cousin et al., 1998). Crystallographic studies on complexes of mouse recombinant, human recombinant, and *Torpedo* AChE with the mamba venom polypeptide neurotoxin fasciculin show that these three enzymes also possess very similar three-dimensional structures (Bourne et al., 1995; Harel et al., 1995; Kryger et al., 1998). Therefore, we investigated the effect of mutation to a smaller residue of the leucine residue in rat AChE equivalent to Leu282 in *Torpedo* AChE, which is either conserved or replaced by valine or methionine, in all of the vertebrate cholinesterases cloned and/or sequenced to date (Table 1; Cousin et al., 1998). We also investigated whether the inherent capacity of *Torpedo* AChE to be deactivated by chemical modification of Cys231 could be conferred on rat AChE by introducing a cysteine moiety in place of the homologous residue, Gly234.

Mutation to alanine of the leucine residue in rat AChE equivalent to Leu282 in *Tm*AChE, viz. Leu289, produced a mutant enzyme, L289(*282*)A[1], that was much more susceptible to thermal denaturation than was the WT enzyme. Arrhenius plots (not shown) revealed that this is associated with a reduction in the energy of activation, from 125 kcal/mol to 90 kcal/mol, a reduction much smaller than that produced by the homologous mutation in *Tm*AChE.

WT rat AChE, as might be expected, is not susceptible to DTP at 26.3°C. However, the G234(*231*)C mutant, in which a cysteine residue has been inserted at a position homologous to that of Cys231 in WT *Tm*AChE, was deactivated, with a $T_{1/2}$ of 30 min, in the presence of 1 mM DTP (data not shown). As might be predicted from the thermal denaturation data for the L289A mutant, the double mutant G234(*231*)C/L289(*282*)A is much more susceptible to DTP under the same experimental conditions and loses activity with a $T_{1/2}$ of ca. 20 min, even in the presence of 0.05 mM DTP (data not shown).

Our initial observation (see above) was a modulation of the stability of the L282S mutant under conditions of the Ellman assay by the prototypic peripheral site ligand *d*-tubocurarine. Therefore, it seemed desirable to conduct a systematic survey of the effects of AChE-specific ligands on the stability of the various mutants discussed above, relative to WT *Tm*AChE. In addition to *d*-tubocurarine and gallamine, which are spe-

TABLE 1
Conservation of residues in the Trp279-Ser291 loop and of residues in domain 2 that interact with this loop

	279	282	286	288	289	291	331	398	399
Torpedo	W	L	S	F	R	S	F	H	N
Rat, mouse	W	L	S	F	R	S	F	H	N
Rabbit	W	L	S	F	R	S	F	H	N
Human	W	L	S	F	R	S	F	H	N
Bovine	W	L	H	F	R	S	F	H	N
Chicken	G	M	S	F	R	A	F	H	N
Quail	G	L	S	F	R	A	F	H	N
Bungarus	W	L	S	F	R	P	F	H	N
Hagfish	G	V	S	F	R	P	F	Y	N
Amphioxus 1	W	V	D	A	D	P	W	P	F
Amphioxus 2	W	W				P	F	Y	N

cific for the peripheral site, edrophonium and tacrine, ligands specific for the "anionic" subsite of the active site (Harel et al., 1993), and decamethonium, a bisquaternary ligand that spans the two sites (Harel et al. 1993), were included for purposes of comparison. IC_{50} values for inhibition of the various *Tc*AChE and rat AChE mutants by these ligands are summarized in Table 2. Not surprisingly, K_m was not greatly influenced by the mutations made in residues near the entrance of the gorge, nor did the C231S mutation influence this parameter. Similarly, only small effects were observed on the IC_{50} values for tacrine and edrophonium, which bind to the anionic subsite of the active site at the bottom of the aromatic gorge. However, the L282S/A and S291G mutations appeared to increase the affinity of *d*-tubocurarine for *Tm*AChE by 2- to 3-fold, whereas they decreased the affinity of gallamine by 4- to 10-fold and of decamethonium by 2- to 3-fold. Whereas the W279A mutation had little effect on the affinity of *d*-tubocurarine and gallamine for *Tm*AChE, it decreased the affinity of decamethonium by about 7-fold. The fact that mutations in the peripheral site region may increase affinity for some peripheral site ligands and decrease that for others is not unusual and may be due to interaction of different peripheral site ligands with diverse sets of amino acid residues (Cousin et al., 1996).

We investigated the effects of the ligands on both thermal denaturation and deactivation produced by chemical modification with DTP for both WT and peripheral site mutants of *Tm*AChE and rat AChE.

For the L282A mutant, the thermal denaturation studies presented a fairly straightforward picture. Edrophonium, tacrine, decamethonium, and gallamine all provided substantial protection against thermal denaturation, whereas *d*-tubocurarine slightly destabilized the enzyme (Fig. 6). The observed protection was reflected in the activation energies calculated from Arrhenius plots obtained in the presence of the various ligands. For the first four ligands, these were substantially higher than the value obtained for L282A in the absence of any ligand. For tacrine (155 kcal/mol), the activation energy approached the value obtained for WT enzyme (170 kcal/mol), and for *d*-tubocurarine, the activation energy was slightly decreased. *d*-Tubocurarine had a similar effect on the W279A mutant (not shown).

Inactivation by DTP presented a more complex picture. At the temperature used, 26.3°C, the WT enzyme was fairly stable, but a slightly increased rate of inactivation was observed in the presence of either *d*-tubocurarine or tacrine (Fig. 7A). For the L282A mutant, gallamine and decamethonium exerted strong protection and edrophonium provided slight protection, whereas *d*-tubocurarine slightly increased the rate of inactivation, and tacrine substantially accelerated inactivation, producing 50% inhibition of enzymic activity within 2 min, as compared with ca. 6 min in its absence (Fig. 7B). Similar results were obtained for S291G, although edrophonium provided greater protection (Fig. 7C). However, for this latter mutant, *d*-tubocurarine enhanced the rate of inactivation (5-fold) much more than did tacrine (2-fold). In the case of W279A, the trend was similar, but the effects were less striking (Fig. 7D). Both gallamine and edrophonium afforded protection, whereas both *d*-tubocurarine and tacrine accelerated deactivation. Similar experiments performed on

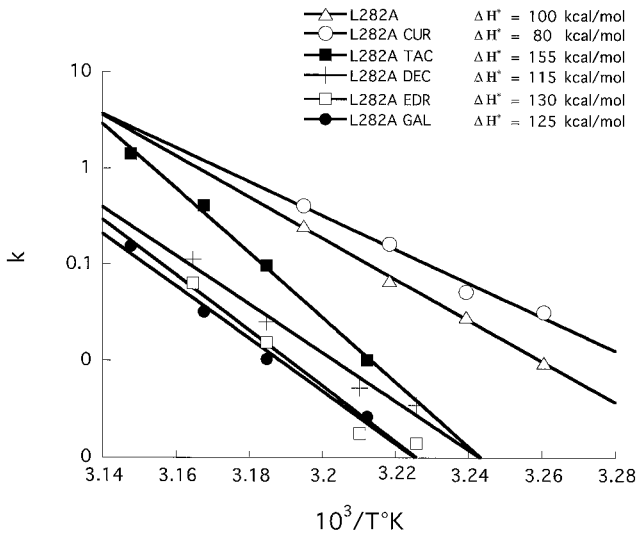

Fig. 6. Activation energies for thermal denaturation of the L282A mutant of *Tm*AChE in the presence and absence of active-site and peripheral-site ligands. Assays were performed and Arrhenius plots were derived as described in the legend to Fig. 5. Ligand concentrations used were: *d*-tubocurarine, 0.5 mM; decamethonium, 20 μM; edrophonium, 10 μM; gallamine, 0.6 mM; tacrine, 100 nM.

TABLE 2

IC_{50} values for inhibition of wild-type and mutant *T. marmorata* and rat AChEs by active and peripheral site ligands

Assay conditions were as described in *Experimental Procedures.*

Enzymes	K_m	IC_{50} Curare	IC_{50} Decamethonium	IC_{50} Edrophonium	IC_{50} Gallamine	IC_{50} Tacrine
	mM			*μM*		
TmAChE						
WT	0.108	170	1.4	0.92	64.2	0.014
L282A	0.152	65	3.6	2.22	398	0.013
W279A	0.199	220	10.7	0.87	118	0.010
S291G	0.172	40	4.7	3.2	375	0.022
C231S	0.074	250	1.3	0.92	98.3	0.013
CS/L282A	0.106	110	3.4	2.1	245	0.014
L282S	0.156	80	4.2	2.0	312	0.017
N280Q	0.098	230	1.7	0.83	118	0.013
NQ/L282S	0.148	64	5.7	2.22	573	0.020
CS/L282S	0.110	90	4.4	2.22	477	0.016
CS/NQ/L282S	0.114	64	5.7	2.74	933	0.020
Rat AChE						
WT	0.085	240	15.4	1.9	1190	0.106
L289A	0.107	120	18	2.6	1430	0.086
G234C		120	30.4	3.2	690	0.112
GC/L289A		60	33.7	4.6	690	0.086

the rat AChE double-mutant G234(*231*)C/L289(*282*)A yielded a rather different pattern of efficacy of ligands. Overall, the effects observed were not striking, but gallamine had a protective effect, decamethonium, *d*-tubocurarine, and edrophonium had little or no effect, and only tacrine enhanced the rate of inactivation substantially, although not as markedly as for the peripheral site mutants of *Tm*AChE (data not shown).

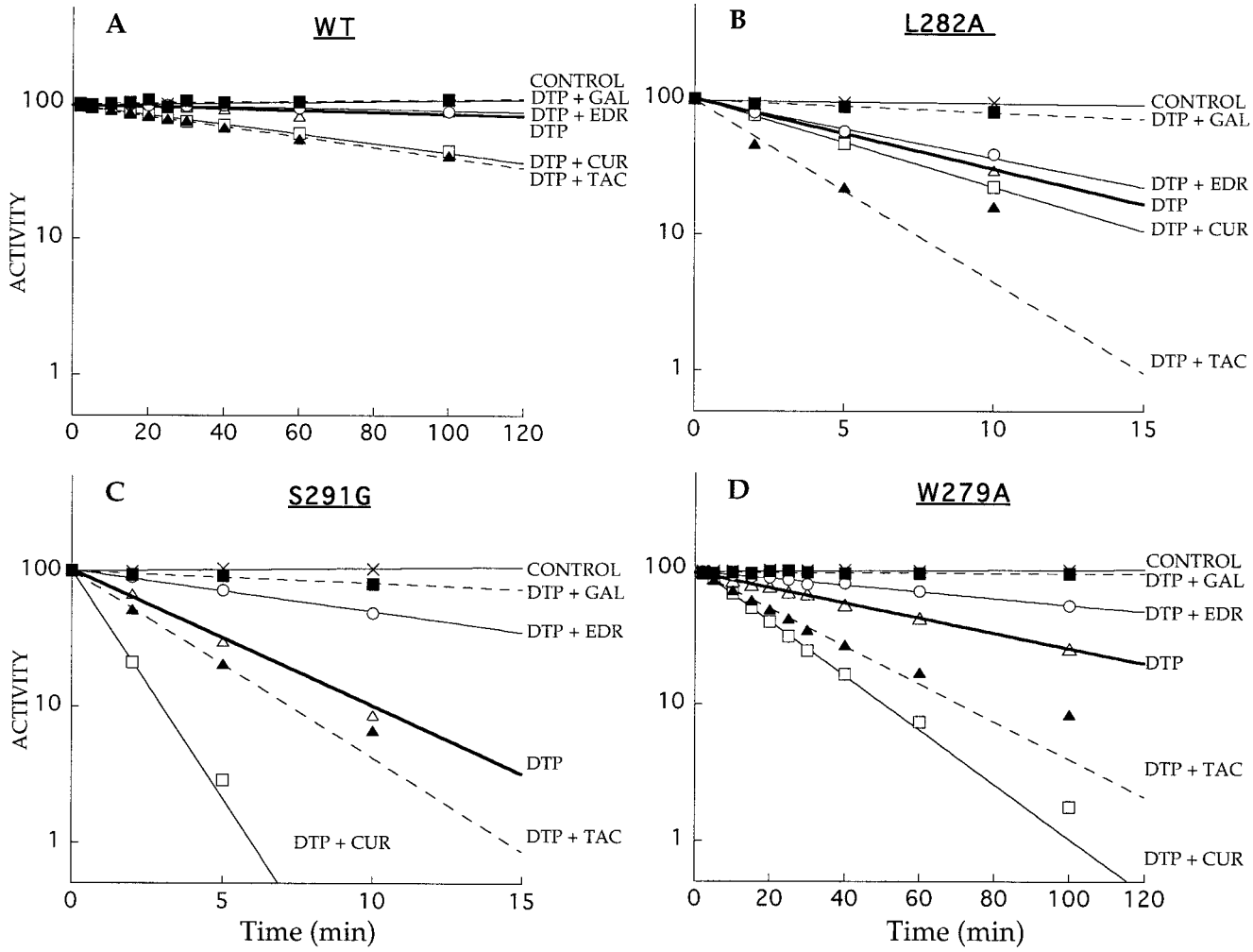

Fig. 7. Effects of active-site and peripheral-site ligands on the kinetics of inactivation of WT *Tm*AChE and the L282A, S291G, and W279A mutants by DTP. The experimental procedure was as described in the legend to Fig. 3. Ligand concentrations used were as described in the legend to Fig. 6. A, WT; B, L282A; C, S291G; and D, W279A.

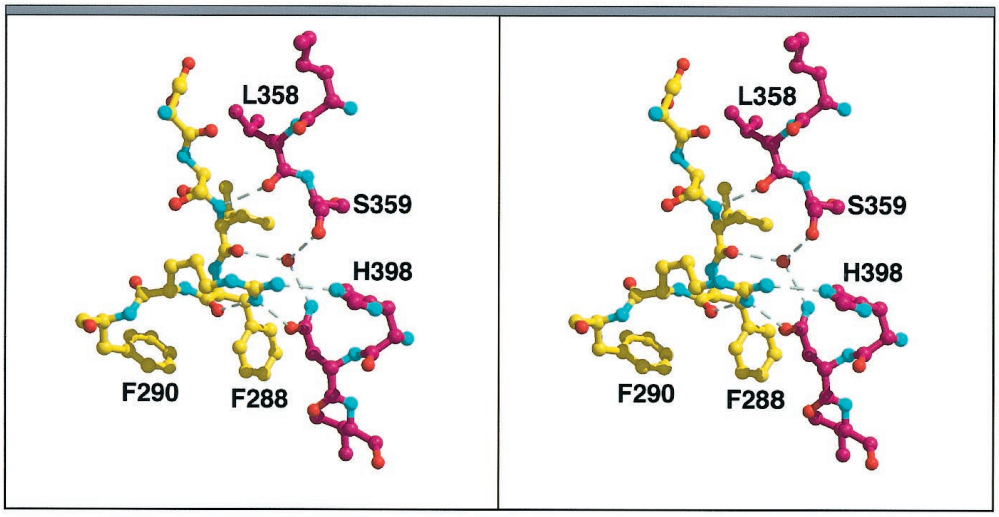

Fig. 8. Stereo figure showing possible hydrogen bonds (dashed lines) between atoms in the Trp279-Ser291 loop (carbon atoms are colored yellow) and domain 2 (carbon atoms are colored purple). Wat555 is the red sphere. Orientation is similar to that shown in Fig. 4 (picture was made in XtalView/Raster3D).

Discussion

Our data are in line with earlier experiments performed on *Tc*AChE, which showed that chemical modification of the nonconserved Cys231 caused a loss of enzymic activity (Steinberg et al., 1990), with concomitant transformation to a partially unfolded state displaying the physicochemical features of a MG state (Kreimer et al., 1994). However, the data concerning mutation of Leu282 add another dimension. Although hydrophobic, this residue is located near the surface of the protein, close to the mouth of the active-site gorge (Fig. 1; Harel et al., 1995). We did not expect that mutation of Leu282, located at the periphery of the protein, would affect so drastically the stability of the entire catalytic subunit containing 537 amino acid residues. There is substantial documentation of studies in which large hydrophobic side chains have been mutated to smaller ones (see, e.g., Yutani et al., 1987; Matsumara et al., 1988; Eriksson et al., 1992b). In general, such mutations destabilize the protein under consideration. In cases where these mutations create empty cavities, the magnitude of the destabilization is greater than in those where the three-dimensional structure adjusts to fill the void created by reducing the size of the side chain (Eriksson et al., 1992b). The proteins so studied have been much smaller than the catalytic subunit of *Tc*AChE, containing up to 268 amino acid residues in the case of the α subunit of tryptophan synthase (Yutani et al., 1987). It was reported that cavity-containing mutants of T4 lysozyme could be stabilized by the uptake of benzene or indole into the cavity (Eriksson et al., 1992a). We were not able to obtain similar stabilization of the L282A mutant by benzene (N. Morel, unpublished observations), probably because in this mutant, the conformation of the loop, and possibly elsewhere, was altered so that no cavity was left after the mutation.

The experimental data presented, whether monitoring loss of enzymic activity due to chemical modification or measuring rates of thermal inactivation and generating Arrhenius plots, are all kinetic. Therefore, at this stage, we cannot differentiate between thermodynamic and kinetic destabilization. Thus, an increase in the rate of thermal inactivation might result from a lowering of the free energy of the intermediate activation state rather than from destabilization of the native state. In any event, the Arrhenius plots reveal that mutations that accelerate the rate of thermal inactivation lower the transition enthalpy (Fig. 5). The effect of ligands on the inactivation of the L282A mutant was not directly correlated with the values of the transition enthalpies observed in their presence (Fig. 8). This suggests that for certain ligands, viz. gallamine, decamethonium, and edrophonium, entropic effects may play a role in stabilization.

To provide a structural basis for the observed destabilization by mutation of Leu282, we have examined the area surrounding the side chain of this residue. Figure 1 shows an overall ribbon view of the enzyme, with the loop containing Leu282 shown in yellow. This figure also shows that the *Tc*AChE can be divided approximately into two halves. By using an older automatic procedure for identifying structural domains in proteins (Wodak and Janin, 1981) and a more recent algorithm (Wernisch et al., 1999), *Tc*AChE is found to consist of two "structural domains," each comprising one contiguous segment of the polypeptide: domain 1 (residues 4–315) and domain 2 (residues 316–357). These domains

TABLE 3
Cross-gorge interactions of residues in the Trp279-Ser291 loop

Source Atom	Target Atoms	Distance Loop-Second Domain
PHE284 CB	PRO361 CB	3.69
PHE284 CG	PRO361 CB	3.97
PHE284 CD2	PRO361 CB	3.90
ASP285 C	LEU358 CD1	3.97
ASP285 O	PRO361 CB	3.97
	LEU358 CD1	3.71
	LEU358 CA	4.03
ASP285 CG	LEU358 CD1	3.54
ASP285 OD1	LEU358 CD1	3.51
ASP285 OD2	LEU358 CD1	3.70
SER286 CA	LEU358 O	3.49
SER286 C	LEU358 O	3.80
SER286 CB	PRO361 CG	3.68
	PRO361 CB	3.70
	LEU358 O	3.84
ILE287 N	LEU358 C	4.07
	LEU358 O	3.16***
ILE287 CA	LEU358 O	4.07
ILE287 C	WAT555 OW	3.74
ILE287 O	WAT555 OW	2.79***
	LEU358 O	3.90
ILE287 CB	LEU358 O	3.89
ILE287 CG1	PHE331 O	3.54
ILE287 CG2	WAT555 OW	4.04
	LEU358 O	4.08
	SER359 OG	3.89
ILE287 CD1	LEU358 CG	3.84
	GLY335 O	3.02
	LEU358 CD2	4.10
	GLY335 CA	3.69
	GLY335 C	3.53
PHE288 CA	PHE331 CD2	4.04
PHE288 O	ASN399 OD1	4.00
PHE288 CB	PHE331 CD2	4.06
	ASN399 CG	3.89
	ASN399 OD1	3.90
	ASN399 ND2	3.71
	WAT555 OW	3.61
PHE288 CG	PHE331 CG	3.95
	PHE331 CD2	3.69
	PHE331 CE2	3.96
	ASN399 CB	3.92
	ASN399 CG	3.57
	ASN399 OD1	3.77
	ASN399 ND2	3.70
PHE288 CD1	PHE331 CE2	4.09
	ASN399 CB	4.08
	ASN399 CG	4.00
	ASN399 OD1	3.92
PHE288 CD2	PHE331 CB	4.01
	PHE331 CG	3.37
	PHE331 CD1	3.55
	PHE331 CD2	3.57
	PHE331 CE1	3.85
	PHE331 CE2	3.90
	PHE331 CZ	4.00
	ASN399 CB	3.63
	ASN399 CG	3.61
	ASN399 ND2	3.53
	VAL395 CG1	3.71
PHE288 CE1	ASN399 CB	4.00
PHE288 CE2	PHE331 CG	3.79
	PHE331 CD1	3.49
	PHE331 CD2	4.02
	PHE331 CE1	3.35
	PHE331 CE2	3.94
	PHE331 CZ	3.58
	ASN399 CB	3.55
	ASN399 CG	4.08
PHE288 CZ	PHE331 CE1	3.81
	PHE331 CE2	4.08
	PHE331 CZ	3.63
	ASN399 CB	3.76
	VAL400 CG2	3.73
ARG289 NE	PRO361 CG	4.02
ARG289 CZ	HIS398 NE2	4.07
	ASN399 OD1	3.92
ARG289 NH1	ASN399 CG	3.91
	ASN399 OD1	2.83***
	WAT555 OW	3.61
ARG289 NH2	PRO361 CD	4.06
	HIS362 ND1	3.97
	HIS362 CE1	3.87
	HIS398 CE1	3.90
	HIS398 NE2	2.96***
	HIS398 CD2	3.85

Asterisks indicate possible hydrogen bonds.

have been defined so as to maximize the interactions between residues within each domain while minimizing the interactions between domains. This definition has been used in many algorithms, with the aim of identifying structural units most likely to fold independently and to be stable on their own (Wetlaufer, 1973). However, this is unlikely to be applicable to the two domains identified in *Tc*AChE, given that they interact strongly with each other and possess a buried surface area of 5070 Å^2, a value nearly three times larger than that in the average protein-protein complex (Janin and Chothia, 1990). Furthermore, the domains represent portions of the α/β hydrolase architecture of AChE that do not seem to represent independent folding motifs found elsewhere. Interestingly, however, our programs detect surprisingly similar domain partitions in other proteins of the α/β hydrolase fold family (Ollis et al., 1992), such as the fungal and pancreatic lipases, that display weak sequence homology with AChE. It is also noteworthy that the members of the catalytic triad of *Tc*AChE, viz. Ser200, Glu327, and His440, come from both domains, and, thus, span the interdomain interface. This is quite common in multidomain enzymes where domain movement plays a role in catalysis (Gerstein

TABLE 4

Possible hydrogen bonds between atoms in the Trp279-Ser291 loop and atoms in domain 2, including Wat555

First Domain		Second Domain	Distance
			Å
Ile287 N		Leu358 O	3.2
Ile287 O	Wat555		2.8
	Wat555	Ser359 O	2.6
	Wat555	Asn399 $N^{\delta 2}$	2.9
Arg289 $N^{\eta 1}$		Asn399 $O^{\delta 1}$	2.8
Arg289 $N^{\eta 2}$		His398 $N^{\varepsilon 2}$	3.0

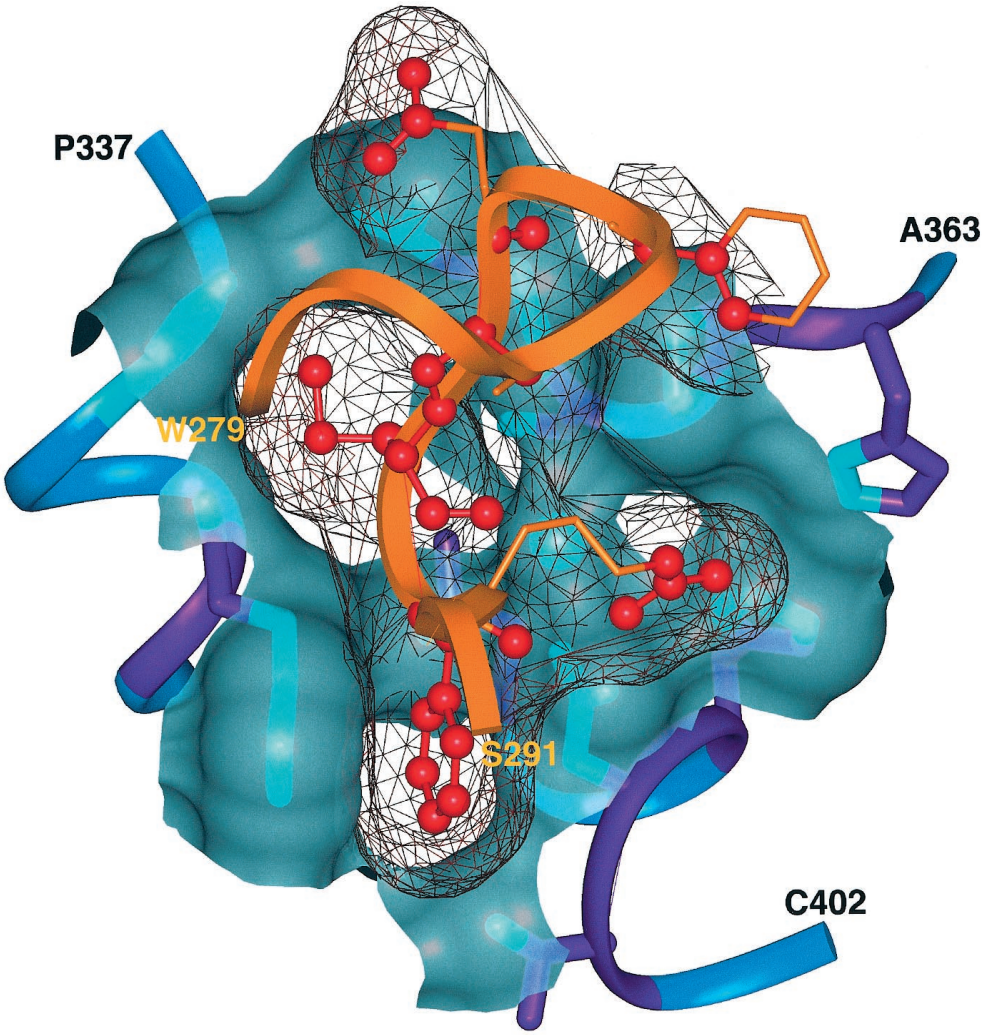

Fig. 9. Interaction of surfaces between the Trp279-Ser291 loop and domain 2. The loop is depicted as an orange ribbon, and only those side chain and main chain atoms that interact with atoms of the second domain (within 4.1Å) are shown. The atoms of those interacting residues that actually make contact are shown as red balls, and the side chain atoms of the same residues that do not make contact are shown in orange stick representations (to provide context and connectivity). The solvent-accessible surface of only the contacting atoms is shown in dark red mesh. The surface is calculated in the context of the entire loop. Relevant residues from domain 2 are shown as three segments of ribbon. Each segment is labeled at its COOH-terminus. Medium blue indicates residues that have no contact with the 279-291 loop. Purple residues have some atoms that contact the loop atoms. Those main chains and side chains of domain 2 that actually contact the loop are colored cyan, and the solvent-accessible surface of these atoms (in the context of the whole second pseudodomain) is shown in light cyan, made transparent to show the atoms of which it is composed. The one cyan sphere is the water molecule, arbitrarily assigned to be part of domain 2 (picture was made in Insight II).

et al., 1994). This suggests that the AChE domains, or, more particularly, their interface, and their counterparts in other α/β hydrolases, might also play a role in enzyme function.

In *Tc*AChE, the interdomain surface involves 548 atoms from a total of 78 residues in domain 1 and 74 residues in domain 2. The interface atoms are defined as those for which the accessible surface area (Lee and Richards, 1971) computed in the entire protein is different from that computed when the domains are considered independently. A sizable portion of the interface residues belongs to loops (52%), with the remainder belonging to helices and strands. It should also be mentioned that 73% of the buried interface area is provided by nonpolar atoms, whereas only 5.5% is contributed by charged atoms. Hence, the interdomain and, thus, also the intergorge interactions are primarily hydrophobic in nature.

TABLE 5
Interactions of side chain atoms of Leu282 with other atoms in the Trp279-Ser291 loop

Atom 1	Atom 2	Distance
		Å
Leu282 C^{γ}	Trp279 O	4.0
	Ser291 O^{γ}	3.9
Leu282 $C^{\delta 1}$	Trp279 $C^{\varepsilon 3}$	4.1
	Ser286 O^{γ}	4.1
	Arg289 O	3.7
	Wat584	3.8
Leu282$C^{\delta 2}$	Pro283 C^{δ}	4.2
	Arg289 C	4.1
	Arg289 O	4.2
	Phe290 N	4.1
	Phe290 C	3.8
	Phe290 O	3.9
	Ser291 N	3.8
	Ser291 C^{α}	3.9
	Ser291 O^{γ}	3.8
	Wat580	4.1

Given the above analysis, visual inspection of Fig. 1 suggests that the loop comprising residues 279 to 291 plays several roles: 1) it makes an important contribution to the peripheral site at the top of the gorge; 2) it participates, via the side chains of residues Phe288 and Phe290, in the acyl binding pocket of the active-site (Harel et al., 1992); and 3) it makes significant cross-gorge interactions with residues in the second domain. To quantify this latter role of the loop, Table 3 lists all of the interactions between residues in the loop and residues in the second domain within a cutoff of 4.1Å. The possible hydrogen bonds formed are displayed in Fig. 8 and listed in Table 4. Table 1 shows that the side chains of the residues involved in these polar cross-domain interactions are well conserved in vertebrate AChE sequences. Consequently, it may be postulated that these residues play a key role in preserving the active conformation of the enzyme and/or in its folding to the native conformation. This prediction could be examined by site-directed mutagenesis studies. Indeed, in preliminary experiments, mutation of Arg289 to glutamate produced an active enzyme that was, however, substantially less stable than WT *Tm*AChE (N. Morel, unpublished observations).

To examine the nonpolar interactions listed in Table 3, Fig. 9 shows the complementarity between the solvent-accessible surfaces of the loop and neighboring atoms in the second domain. Of particular interest is the sandwiching of the loop residue Phe288 between the side chains of Phe331 and Asn399, both of domain 2. Also noteworthy is the fact that Ile287 buries 140 $Å^2$ in the interface, the second largest value after Phe448 (not interacting with the loop), which buries 164 $Å^2$. In all, the loop buries approximately 446 $Å^2$ of surface area in the interaction between the two domains.

The participation of residues in the Trp279-Ser291 loop in cross-gorge interactions implies that destabilization of the loop itself would perturb important interdomain interactions, thereby impairing the activity and, possibly, also the stabil-

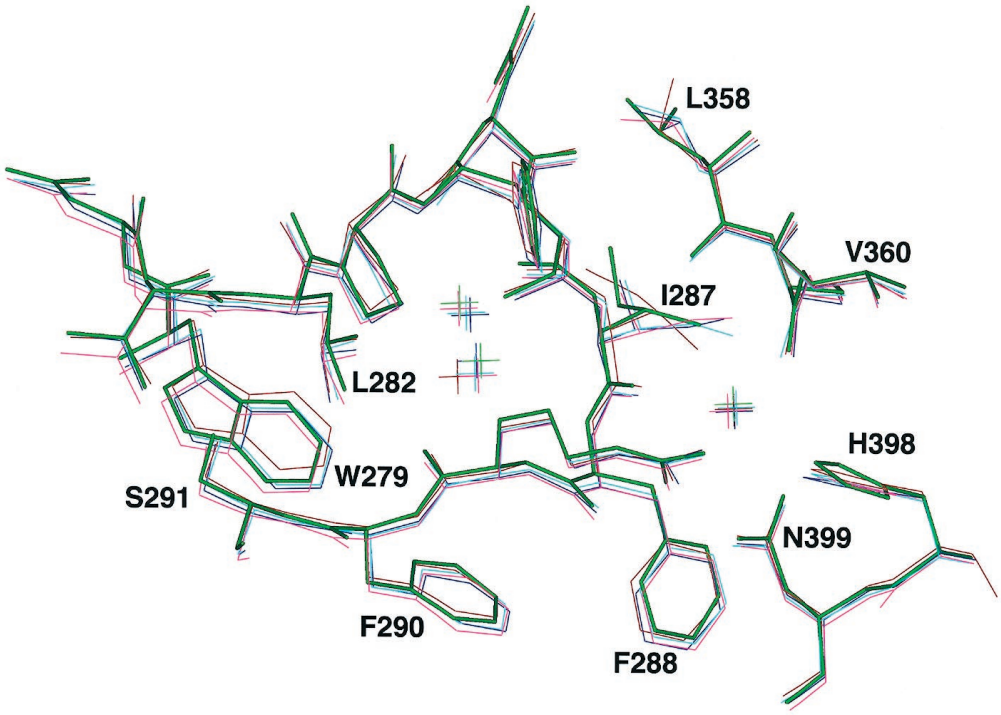

Fig. 10. Overlay of five AChE crystal structures in the region of the Trp279-Ser291loop. The structures used are as follows: soman-inactivated (Millard et al., 1998; green); complex with huperzine A (Raves et al., 1997; PDB entry 1vot; dark blue); complex with edrophonium (Harel et al., 1993; PDB entry 1ack; cyan), sarin-inactivated (Millard et al., 1998; dark pink); and native AChE (Raves et al., 1997; PDB entry 2ace; brown). Overlap of structures is based on the assumption that all five of the crystals are isomorphous. The overlay shows that there are no large qualitative differences in the conformation of the loop, despite the presence or absence of inhibitors at the bottom of the active-site gorge. The largest differences are exhibited by the side chains of Ile287 and Leu358, which appear to adopt a number of different conformations. Furthermore, 2ace lacks one water molecule, uppermost in the representation (picture was made in Insight II).

ity of the entire subunit. The side chain of Leu282 is almost completely buried, with only 10 Å^2 of surface area exposed to solvent. Figure 4 shows that it fills the central cavity of this loop, making van der Waals interactions with other atoms in the vicinity (Table 5 and Fig. 10). Furthermore, we see that Phe288 adopts a left-handed helical backbone conformation, usually associated with glycine and asparagine residues. Thus, decreasing the size of the side chain of Leu282, as in the L282A mutant, would most probably change the conformation of the loop or increase its conformational flexibility. Consequently, this would compromise the cross-gorge interactions shown in Figs. 8 and 9, resulting in the observed loss of activity and the surmised loss of stability. Similar considerations would apply to the destabilization achieved by analogous substitution of Trp279 and Ser291 by amino acids with smaller side chains. However, although the destabilization produced by the S291G mutation is rather similar to that produced by the L282S or L282A mutation, that produced by the W279A mutation is much smaller. This difference may tentatively be ascribed to the fact that the principal interaction of Leu282 is with Ser291, and vice versa, both side chains being almost completely buried. As can be seen from Table 5, Ser291O$^{\gamma}$ makes van der Waals contacts with both Leu282C$^{\gamma}$ and L282C$^{\delta 2}$. In the case of Trp279, the indole ring, although hydrophobic, is largely oriented outwards, toward the active-site gorge, where it is available for interaction with peripheral site ligands (Harel et al., 1992, 1993, 1995; Bourne et al., 1995) and it makes a single, weaker interaction via its C$^{\epsilon 3}$ atom with Leu282C$^{\delta 1}$. It is of interest that within the loop, two buried waters, Wat580 and Wat584, appear to contribute to stabilization via van der Waals interactions and hydrogen bonds.

The effects of the various reversible inhibitors on the stability of the mutant enzyme(s) are also of interest, although for the peripheral site ligands, no crystallographic data are available to reveal details of their interaction with the AChE, and it would be difficult to obtain meaningful assignments from docking studies. This was evident from comparison of the X-ray structures of complexes, e.g., of fasciculin/AChE (Harel et al., 1995) and of huperzine A/AChE (Raves et al., 1997), with the structures predicted by docking. The data for thermal denaturation of the L282A reveal that all of the ligands examined, whether peripheral, active-site directed, or spanning the two sites, stabilize the protein, with the exception of *d*-tubocurarine, the destabilizing effect of which was the starting point for the current study. In general, the binding energy conferred by a ligand might be expected to stabilize the structure of a protein unless it binds better to the transition state for unfolding than to the native ground state. The data obtained on the effect of the various ligands on chemical deactivation by DTP are rather unexpected. Again, it was found that edrophonium and gallamine retard deactivation, in agreement with our earlier observation that edrophonium retarded inactivation of *Tc*AChE by *N*-ethylmaleimide and *p*-chloromercurisulfonic acid (Steinberg et al., 1990). Our finding that both the peripheral site ligand, *d*-tubocurarine, and the active-site ligand, tacrine, enhance the rate of inactivation, and that the latter has a strong effect on the rates of inactivation of L282A, S291G, and W279A, was quite unexpected. We earlier showed that *N*-methylacridinium, the structure of which is rather similar to that of tacrine and which, presumably, interacts with the anionic site at the bottom of the active-site gorge in a similar way (Harel et al., 1993), does not affect chemical modification of *Tc*AChE by *N*-ethylmaleimide (Steinberg et al., 1990). Furthermore, Abramson et al. (1989) found no effect of this ligand on the irreversible modification of *Tc*AChE by the molluscan toxin onchidal. Indeed, in our present study, we found that tacrine has little effect on chemical modification of WT *Tm*AChE. Because tacrine protects L282A against thermal denaturation, it must be speculated that its binding to the mutant enzyme produces a conformational change that renders the sulfhydryl group of Cys231 more accessible to chemical modification.

As presented in *Results*, comparison of the effect of the same set of ligands on susceptibility of the rat G234(*231*)C and G234(*231*)C/L289(*282*)A mutants to chemical modification revealed broad overall similarity to what was observed with the corresponding *Torpedo* mutants. However, it is of interest that *Bungarus fasciatus* AChE is much less susceptible to propidium and gallamine than the *Torpedo* enzyme, but slightly more susceptible to *d*-tubocurarine (Cousin et al., 1996), as is also the case for the L282A/S and S291G *Tm*AChE mutants relative to the WT (see Table 2). In the absence of crystallographic data, it is premature to attempt to rationalize these different patterns of susceptibility.

The experimental data presented, taken together with the theoretical analysis, show how mutation of a single residue at the periphery of a relatively large native protein structure can affect its overall stability.

Acknowledgments

This study was supported by Centre National de la Recherche Scientifique; Direction des Systèmes de Force et de la Prospective; Association Française contre les Myopathies; Fourth Framework Program in Biotechnology of the European Union; U.S. Army Research and Materiel Command under Contract 17-97-2-7022; Kimmelman Center for Biomolecular Structure and Assembly; and Concerted Research Action Program of the French Community of Belgium (Contract 97/02-211). The expert technical assistance of Anne Le Goff is gratefully acknowledged, as is the participation of Philippe Chanal and Charles J. Waechter in the early stages of the project. I. S. is the Bernstein-Mason Professor of Neurochemistry.

References

Abramson SN, Radic Z, Manker D, Faulkner DJ and Taylor P (1989) Onchidal: A naturally occurring irreversible inhibitor of acetylcholinesterase with a novel mechanism of action. *Mol Pharmacol* **36:**349–354.

Alard P (1992) Calculs de surface et d'énergie dans le domaine de macromolécules (Ph.D. Thesis). Brussels, Belgium: Free University of Brussels, 120 p.

Bourne Y, Taylor P and Marchot P (1995) Acetylcholinesterase inhibition by fasciculin: Crystal structure of the complex. *Cell* **83:**503–512

Changeux, J-P (1966) Responses of acetylcholinesterase from *Torpedo marmorata* to salts and curarizing drugs. *Mol Pharmacol* **2:**369–392.

Collaborative Computational Project, Number 4 (1994) The CCP4 Suite: Programs for Protein Crystallography. *Acta Crystallogr Sect D Biol Crystallogr* **50:**760–763.

Cousin X, Bon S, Duval N, Massoulié J and Bon C (1996) Cloning and expression of acetylcholinesterase from *Bungarus fasciatus* venom. *J Biol Chem* **271:**15099–15108.

Cousin, X., Hotelier T, Giles K, Toutant J-P and Chatonnet A (1998) aCHEdb: The database system for ESTHER, the α/β fold family of proteins and the Cholinesterase gene server. *Nucleic Acids Res* **26:**226–228.

De Ferrari GV and Inestrosa NC (1998) Identification of an acetylcholinesterase fragment that promotes Alzheimer β-amyloid fibril formation, in *Structure and Function of Cholinesterases and Related Enzymes* (Doctor BP, Quinn DM, Rotundo RL and Taylor P eds) pp 185–186. Plenum Press, New York.

Delhaise P, Bardiaux M and Wodak SJ (1984) Interactive computer animation of macromolecules. *J Mol Graphics* **2:**103–106.

Duval N, Massoulié J and Bon S (1992) H and T subunits of acetylcholinesterase from *Torpedo*, expressed in COS cells, generate all types of globular forms. *J Cell Biol* **118:**641–653.

Ellman GL, Courtney KD, Andres V Jr and Featherstone RM (1961) A new and rapid determination of acetylcholinesterase activity. *Biochem Pharmacol* **7:**88–95.

Eriksson AE, Baase WA, Wozniak JA and Matthews BW (1992a) A cavity-containing

mutant of T4 lysozyme is stabilized by a buried benzene. *Nature (London)* **355:** 371–373.
Eriksson AE, Baase WA, Zhang X-J, Heinz DW, Blaber M, Baldwin EP and Matthews BW (1992b) Response of a protein structure to cavity-creating mutations and its relation to the hydrophobic effect. *Science (Wash DC)* **255:**178–183.
Gerstein M, Lesk A and Chothia C (1994) Structural mechanisms for domain movement in proteins. *Biochemistry* **33:**6739–6749.
Harel M, Kleywegt GJ, Ravelli RBG, Silman I and Sussman JL (1995) Crystal structure of an acetylcholinesterase-fasciculin complex: Interaction of a three-fingered toxin from snake venom with its target. *Structure* **3:**1355–1366.
Harel M., Schalk I, Ehret-Sabatier L, Bouet F, Goeldner M, Hirth C, Axelsen PH, Silman I and Sussman JL (1993) Quaternary ligand binding to aromatic residues in the active-site gorge of acetylcholinesterase. *Proc Natl Acad Sci USA* **90:**9031–9035.
Harel M, Sussman, JL, Krejci E, Bon S, Chanal, P, Massoulié, J and Silman, I (1992) Conversion of acetylcholinesterase to butyrylcholinesterase: Modeling and mutagenesis. *Proc Natl Acad Sci USA* **89:**10827–10831.
Inestrosa NC, Alvarez A, Pérez CA, Moreno RD, Vicente M, Linker C, Casanueva OI, Soto C and Garrido J (1996) Acetylcholinesterase accelerates assembly of amyloid-β-peptides into Alzheimer's fibrils: Possible role of the peripheral site of the enzyme. *Neuron* **16:**881–891.
Janin J and Chothia C (1990) The structure of protein-protein recognition sites. *J Biol Chem* **265:**16027–16030.
Kreimer DI, Dolginova EA, Raves M, Sussman JL, Silman I and Weiner L (1994) A metastable state of *Torpedo californica* acetylcholinesterase generated by modification with organomercurials. *Biochemistry* **31:**12248–12254.
Kryger G, Giles K, Harel M, Toker L, Velan B, Lazar A, Kronman C, Barak D, Ariel N, Shafferman A, Silman I and Sussman JL (1998) 3D structure studies of a complex of human recombinant acetylcholinesterase with fasciculin-II at 2.7 Å resolution, in *Structure and Function of Cholinesterases and Related Enzymes* (Doctor BP, Quinn DM, Rotundo RL and Taylor P eds) pp 323–326, Plenum Press, New York.
Lee BK and Richards FM (1971) The interpretation of protein structures: Estimations of static accessibility. *J Mol Biol* **55:**379–400.
Legay C, Bon S and Massoulié J (1993) Expression of a cDNA encoding the glycolipid-anchored form of rat acetylcholinesterase. *FEBS Lett* **315:**163–166.
Massoulié J, Sussman JL, Doctor BP, Soreq H, Velan B, Cygler M, Rotundo R, Shafferman A, Silman I and Taylor P (1992) Recommendations for nomenclature in cholinesterases, in *Multidisciplinary Approaches to Cholinesterase Functions* (Shafferman A and Velan B eds) pp 285–288, Plenum Press, New York.
Matsumara M, Becktel WJ and Matthews BW (1988) Hydrophobic stabilization in T4 lysozyme determined directly by multiple substitutions of Ile 3. *Nature (London)* **334:**406–410.
McRee DE (1992) A visual protein crystallographic software system for X11/XView. *J Mol Graphics* **10:**44–46.
Merritt EA and Bacon, DJ (1997) Raster3D: Photorealistic molecular graphics. *Methods Enzymol* **277:**505–524.
Millard CB, Kryger G, Ordentlich A, Harel M, Raves ML, Greenblatt H, Segall Y, Barak D, Shafferman A, Silman I and Sussman JL (1998) Crystal structures of "aged" phosphorylated and phosphonylated acetylcholinesterase, in *Structure and Function of Cholinesterases and Related Enzymes* (Doctor BP, Quinn DM, Rotundo RL and Taylor P eds) pp. 425–432. Plenum Press, New York.
Ollis DL, Cheah E, Cygler M, Dijkstra B, Frolow F, Franken SM, Harel M, Remington SJ, Silman I, Schrag J, Sussman JL, Verschueren KHG and Goldman A (1992) The α/β hydrolase fold. *Protein Eng* **5:**197–211.
Raves ML, Harel M, Pang Y-P, Silman I, Kozikowski AP and Sussman JL (1997) Structure of acetylcholinesterase complexed with the nootropic alkaloid, (−)-huperzine A. *Nat Struct Biol* **4:**57–63.
Richards FM (1974) The interpretation of protein structures: Total volumes, group volumes distribution, and packing density. *J Mol Biol* **82:**1–14.
Shin I, Silman I and Weiner LM (1996) Interaction of partially unfolded forms of *Torpedo* acetylcholinesterase with liposomes. *Protein Sci* **5:**42–51.
Steinberg N, Roth E and Silman I (1990) *Torpedo* acetylcholinesterase is inactivated by thiol reagents. *Biochem Int* **21:**1043–1050.
Sussman JL, Harel M, Frolow F, Oefner C, Goldman A, Toker L and Silman I (1991) Atomic structure of acetylcholinesterase from *Torpedo californica*: A prototypic acetylcholine-binding protein. *Science (Wash DC)* **253:**872–879.
Wernisch L, Hunting M and Wodak SJ (1999) Identifying structural domains in proteins by a graph heuristic. *Proteins* **35:**338–352.
Wetlaufer DB (1973) Nucleation, rapid folding, and globular intrachain regions in proteins. *Proc Natl Acad Sci USA* **70:**679–701.
Wilson EJ, Massoulié J, Bon S and Rosenberry TL (1996) The rate of thermal inactivation of *Torpedo* acetylcholinesterase is not reduced in the C231S mutant. *FEBS Lett* **379:**161–164.
Wodak SJ and Janin, J (1981) Location of structural domains in proteins. *Biochemistry* **20:**6544–6552.
Yutani K, Ogasahara K, Tsujita T and Sugino, Y (1987) Dependence of conformational stability on hydrophobicity of the amino acid residue in a series of variant proteins substituted at a unique position of tryptophan synthase α subunit. *Proc Natl Acad Sci USA* **84:**4441–4444.

Send reprint requests to: Dr. Israel Silman, Department of Neurobiology, Weizmann Institute of Science, Rehovoth 76100, Israel. E-mail: bnsilm@weizmann.weizmann.ac.il